A Novel Adaptive, Real-Time Algorithm to Detect Gait Events From Wearable Sensors

Noelia Chia Bejarano, Emilia Ambrosini, Alessandra Pedrocchi, Giancarlo Ferrigno, *Member, IEEE*, Marco Monticone, and Simona Ferrante

I. Introduction

DURING the rehabilitation of neurological patients, task-oriented, repetitive, immersive exercises along with enriched sensorial feedback are crucial elements in the stimulation of activity-dependent central nervous system plasticity, thereby facilitating motor relearning [1]–[4].

The recovery of gait is the main objective of lower limb rehabilitation [5]. To maximize the efficacy of gait interventions, real-time information correlated to the movement can be exploited. The knowledge of such information would allow the design of real-time feedbacks highly correlated to the patient-specific task deficits or the use of systems to augment proprioceptive inputs, such as electrical or mechanical stimulation, synchronized with the gait cycle [2], [4], [6].

Wearable sensors have proven to be the optimal sensor solution in providing meaningful real-time information correlated to locomotion [7]. Their reduced size and cost allow for both clinical settings and home environment applications. The most widely used sensors are accelerometers, which are capable of monitoring over-ground gait with low power consumption [7]. However, their signal is affected by heel-strike vibrations and is characterized by an inter-session reliability dependent on their orientation with respect to the body segment and on the distance between the sensor and the center of rotation of the joint. The combination of accelerometers with gyroscopes (inertial sensors) can mitigate some of these problems, reducing the monitoring errors. However, both sensors suffer from drift problems when integrated, which can be held down by *ad hoc* signal processing [7].

An alternative solution to inertial sensors are force sensitive resistors, such as footswitches. Their output is very easy to process but they do not provide any information regarding the swing phase of the gait. They also have been reported to cause some discomfort, be prone to mechanical failure, and sometimes be unreliable when worn by patients with drop foot or shuffling feet [8], [9].

Finally, body-mounted Inertial and Magnetic Measurement Systems (IMMSs), combining data from tri-axial gyroscopes, accelerometers and magnetometers, seem to be a more stable solution for prolonged applications [7]. A Kalman filter, embedded in some commercial IMMSs, is used to correct the drift and to provide data fusion to increase sensor accuracy. However, the inclusion of the magnetometer implies that the environment in which they are used needs to be controlled, since they are affected by magnetic interferences.

Nevertheless, IMMSs have been receiving increased interest in the neurorehabilitation field. They have been used in the assessment of the training effects as a portable alternative to traditional gait analysis systems [10]–[12]. Among others, the Outwalk protocol [12] used IMMSs to accurately obtain the thorax, pelvis, and lower-limbs 3-D kinematics during the gait of children with cerebral palsy and amputees. The neurorehabilitation field has also been recently enriched by the development of novel methods to detect gait events using inertial sensors or

Manuscript received February 19, 2014; revised May 29, 2014; accepted June 15, 2014. This work was supported in part by the Italian Ministry of Education, Universities and Research under Grant 2010R277FT ("Fall Risk Estimation and Prevention in the elderly using a Quantitative multifactorial Approach"). Date of publication July 22, 2014; date of current version May 06, 2015.

N. Chia Bejarano, A. Pedrocchi, G. Ferrigno, and S. Ferrante are with the Neuroengineering and Medical Robotics Laboratory, Department of Electronics, Information and Bioengineering, Politecnico di Milano, 20133, Milan, Italy (e-mail: noelia.chia@polimi.it).

E. Ambrosini is with the Neuroengineering and Medical Robotics Laboratory, Department of Electronics, Information and Bioengineering, Politecnico di Milano, 20133, Milan, Italy, and also with the Physical Medicine and Rehabilitation Unit, Scientific Institute of Lissone, Salvatore Maugeri Foundation, Institute of Care and Research, IRCCS, Lissone, Monza Brianza, Italy.

M. Monticone is with the Physical Medicine and Rehabilitation Unit, Scientific Institute of Lissone, Salvatore Maugeri Foundation, Institute of Care and Research, IRCCS, Lissone, Monza Brianza, Italy.

Color versions of one or more of the figures in this paper are available online.

IMMSs, which can be offline or real-time methods. The offline algorithms have been typically used for assessment, exploiting signal conditioning techniques, such as wavelet [8] or Fourier analysis coupled with derivatives [13], [14], and integration [9], to improve the detection of gait events. More recently, inertial sensors and IMMSs have been used to extract the gait events in real time, which can be exploited during gait training [15]–[18]. Online algorithms generally low-pass filter the signals to prepare them for integration [15] or detection of peaks related to gait events [15], [17], [18]. These algorithms are usually tailored on a specific set of data acquired from a restricted population sample (i.e., young and healthy subjects [17], [19] or patients with a specific pathology [16]). The use of precollected data in the design of algorithms enhances their performance, but strongly limits their generalizability to new sets of data. Moreover, the online algorithms proposed so far are affected by small but systematic detection delays due to the use of low-pass filters that improve the online peak detection. New methods have been proposed using more complex techniques such as continuous wavelet transforms [20], which increased accuracy at the expense of a higher detection delay.

The aim of this study was to design an adaptive algorithm capable of providing accurate gait-event detection in real time, to allow the development of novel motor relearning treatments for neurological patients. The developed algorithm was validated against an already established commercial system, using data collected on 22 healthy subjects, both young and elderly adults. The algorithm's performance was then statistically compared to other online algorithms proposed in the literature. Finally, its robustness against sudden speed changes and neurological gait patterns was assessed.

II. Materials and Methods

A. Algorithm Design

The algorithm used two sensors, placed laterally, one on each shank. The number of sensors and their placement was optimized in a previous study [21] in which eight IMMS sensors were analyzed, placed on both lower limbs (insteps, shanks, and thighs), S1 vertebra, and chest. This study selected the two sensors placed on the shanks based on a tradeoff between system portability (minimization of the number of sensors), inter-subject variability, and high correlation between signals and gait events.

The shank angular velocity in the sagittal plane and the shank flexion/extension angle (referred to the vertical axis) were used to detect three gait events per leg: Initial Contact (IC), End Contact (EC), and Mid-Swing (MS). IC was defined as the minimum of the flexion/extension angle, whereas EC and MS were defined as the minimum and the maximum of the angular velocity, respectively (Fig. 1). The complete set of gait events defined six gait phases that are shown in Fig. 1:

1) the right/left double support, between the right/left IC and the left/right EC (phases 1/4);
2) the left/right initial swing, between the left/right EC and the left/right MS (phases 2/5);
3) the left/right terminal swing, between the left/right MS and the left/right IC (phases 3/6).

The definition of the gait events was made by comparing the acquired signals to the IC and EC gait events provided by the GaitRite system and taking into account what was already suggested in the literature [8]. The definition of the EC and MS events was consistent with the literature; in the case of IC, the minimum in the flexion/extension angle was preferred to the minimum of the angular velocity suggested by Aminian *et al.* [8] since it provided lower detection delays and a higher accuracy. In addition to the IC, EC, and MS events, one extra point of interest was used, referred to as ANgle (AN, see Fig. 1). The AN was defined as the value of the flexion/extension angle corresponding to the EC detection. A threshold based on previous AN values was used to trigger the search for the next EC event.

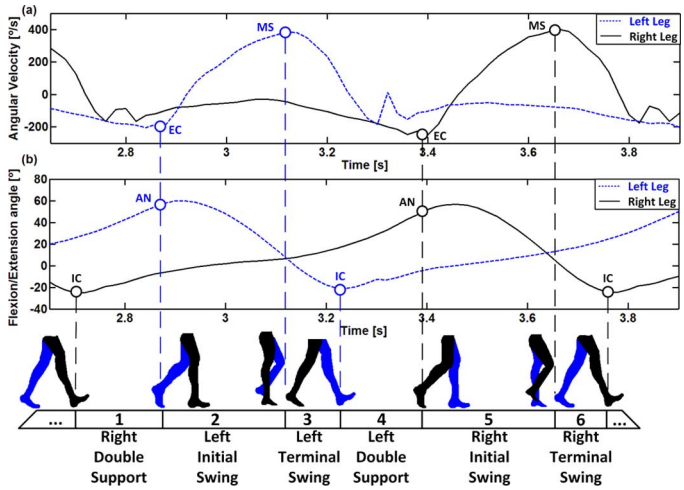

Fig. 1. (a) Shank sagittal-plane angular velocity and (b) flexion/extension angle for the left (dashed blue) and right (solid black) legs. Initial Contact (IC), End Contact (EC) and Mid-Swing (MS) defined the six gait phases. Point Angle (AN), used in the detection of EC, is also shown.

The algorithm consisted of three stages that ran automatically with no input required from the operator: calibration, real-time detection, and step-by-step update.

1) Calibration: When the subject started walking, the first five steps were analyzed on the fly to determine the initial values of the algorithm parameters (i.e., the thresholds defined for the detection of MS, IC, EC, and AN, whose calculation is detailed in the Appendix). These values were then used during the real-time detection, which started immediately after.

2) Real-Time Detection: The core of the algorithm was the real-time gait detection stage which was based on a state machine where the states were the six gait phases shown in Fig. 1. The four signals of interest were initially low-pass filtered with a first-order low-pass FIR filter with a cutoff frequency of 14 Hz. This filter was designed to find a compromise between high frequency noise reduction and low filter delay. Subsequently, the algorithm identified, independently for the left and right leg, the gait events (IC, EC, MS) when the signal peaks overcame the corresponding thresholds while occurring in the expected state.

3) Update: The update stage ran simultaneously to the real-time detection, and it complemented it by updating the thresholds using the newest correct gait events. In this stage, the signals were processed with a 10th order low-pass equiripple FIR filter with linear phase and cutoff frequency of 4 Hz, thus providing a quasi real-time gait event detection that was delayed but more reliable with respect to the real-time detection. The filter was designed after an offline analysis of the Fourier transform

of the signals of interest acquired from all the subjects participating in this study. The quasi real-time detection of the last five steps was used to update the thresholds at every step and to modify the current state when an error occurred. This solution was introduced in order to minimize the detection delay and simultaneously avoid the error propagation.

For the four points of interest (MS, EC, IC, AN) different procedures based on statistical methods were applied to compute the thresholds. Further details regarding the calculation of the thresholds and the algorithm design are reported in the Appendix.

B. Validation of the Algorithm

Twenty-two healthy subjects were recruited (8 males, 14 females; mean age of 47.8 $\pm$ 22.4 years old, range from 21 to 85 years old; mean height of 1.69 $\pm$ 0.08 m; mean weight of 60.9 $\pm$ 9.9 kg). Three IMMSs sampled at 50 Hz (MTx sensors from Xsens Technologies B.V., Netherlands) were placed on the S1 vertebra and on the midpoint of the external part of both shanks, using Velcro and double-sided adhesive tape. The sensors on the shanks were aligned with the longitudinal axis of the limbs. The sensor placed on S1 was used to make a comparison with a previously published algorithm [15]. At the beginning of each session, the subjects were asked to keep an upright standing position for a few seconds in order to create a common global reference system for all inertial and magnetic sensors [22]. This procedure also compensated for possible misalignments between the sensor and the longitudinal axis of the shank. The acquisition was synchronized with the GaitRite system (CIR Systems Inc., United States), using the synchronization output built into the GaitRite. The GaitRite system was used as ground truth, because it is widely used in the clinics and several studies have reported its validity providing spatio-temporal gait parameters, comparing them against motion captures system based on video cameras [23], [24]. The data acquired through the GaitRite were sampled at 120 Hz. Subjects were asked to walk over the GaitRite mat (4.88 m length) at three different self-selected speeds: slow, normal, and fast. Each condition was repeated 12 times, each time including three strides before and after the mat, allowing subjects to maintain a constant speed over the mat.

The algorithm validation was performed in terms of accuracy and timing agreement, comparing all of the first and last contacts of the feet with the GaitRite system against the IC and EC events detected by the proposed real-time algorithm. Only the steps completely executed on the GaitRite walkway were included in the validation.

The accuracy was assessed using the metrics Precision (P), Recall (R), and F1-score, defined as function of True Positives (TP), False Positives (FP), and False Negatives (FN).

$$P = \frac{TP}{(TP + FP)}$$
$$R = \frac{TP}{(TP + FN)}$$
$$F1 = \frac{2PR}{(P + R)}. \quad (1)$$

For the timing agreement, the Bland-Altman method [25] was used to compare the instants at which the gait events (IC, EC) were detected by the two systems. The timing differences between the detection instants were computed, and the agreement was characterized in terms of mean values, 95% confidence intervals, and limits of agreement (mean $\pm$ 1.96 standard deviation). Positive timing differences corresponded to delays in the detection of the real-time algorithm with respect to the GaitRite system.

Two already published algorithms [15], [17] were implemented and validated against the GaitRite system in terms of accuracy (precision, recall, F1-score) and timing agreement (Bland-Altman method), and the results were compared to those of the real-time algorithm proposed here. Lee's algorithm [17] used the shank sagittal-plane angular velocity, where IC and EC were located as minima of the signal low-pass filtered at 3 Hz. The detection of both events depended on the extraction of MS, thus introducing a critical delay in the case of EC. González's algorithm [15] used the anterior–posterior and vertical accelerations extracted from the S1 vertebra, where IC and EC were maxima and minima, respectively, of those signals. The detection of both events was triggered after finding zero-crosses on the anterior–posterior acceleration low-pass filtered at 2 Hz, which introduced delays that were higher in the case of IC.

For the timing agreement, a statistical analysis was performed to compare the performance of the three algorithms in terms of detection delays of IC and EC. A Kolmogorov-Smirnov test demonstrated that the data were not normally distributed. Therefore, six nonparametric Kruskal-Wallis tests ($p < 0.05$) were performed, and each event (IC, EC) and speed condition (slow, normal, fast) were analyzed separately. Dunn-Sidak *post hoc* tests ($p < 0.05$) were used to determine which pairs of effects were significantly different.

C. Robustness of the Algorithm

Two additional experimental validations were performed to test the algorithm's robustness against sudden speed changes and neurological gait patterns. The first one verified if the algorithm could rapidly adapt the threshold values to changes in the peaks amplitudes and latency. The test on neurological patients was designed to establish if the real-time algorithm was robust to a high inter-step variability that can be very likely in stroke patients.

1) Influence of Sudden Changes in Pace: This first experimental validation included ten healthy subjects belonging to the validation group (10 females; mean age of 25.1 $\pm$ 4.6 years old, range from 21 to 34 years old; mean height of 1.69 $\pm$ 0.05 m; mean weight of 57.2 $\pm$ 9.4 kg) who were asked to walk over the GaitRite mat, wearing two IMMSs sensors attached to their shanks. The subjects were instructed to start walking at a slow speed for a few steps and to progressively increase it; and vice versa: to start walking at a fast speed and to progressively decrease it. Both tasks were repeated five times. Each repetition included a few steps before and after the mat, to make the task easier. The execution order of the two tasks was randomized among subjects. As previously described, the calibration of the algorithm parameters was based on the five initial steps, meaning that steps at slow speed were used in the slow-to-fast

TABLE I
PERFORMANCE OF THREE ALGORITHMS (REAL TIME, LEE AND GONZALEZ) IN TERMS OF TRUE POSITIVES (TP), FALSE POSITIVES (FP), FALSE NEGATIVES (FN), AND F1-SCORE

		Initial Contact			End Contact		
		RT	Lee	Gonz	RT	Lee	Gonz
Slow speed	TP	1706	1706	1699	1706	1706	1698
(N=1706,	FP	0	0	3	0	0	6
speed=1.11	FN	0	0	7	0	0	8
± 0.19 m/s)	F1	1	1	0.997	1	1	0.996
Normal	TP	1579	1579	1544	1579	1579	1539
speed	FP	0	0	1	0	0	6
(N=1579,	FN	0	0	35	0	0	40
speed=1.31	F1	1	1	0.989	1	1	0.985
± 0.23 m/s)							
Fast speed	TP	1394	1394	1393	1394	1394	1388
(N=1394,	FP	0	0	26	0	0	23
speed=1.74	FN	0	0	1	0	0	6
± 0.25 m/s)	F1	1	1	0.990	1	1	0.990

tests, whereas steps at high speed were used in the fast-to-slow tests. The accuracy (precision, recall, F1-score) and timing agreement (Bland-Altman method) for both IC and EC were computed.

2) Influence of Pathological Gait Pattern: Ten stroke patients (7 males, 3 females; mean age of 69.4 ± 12.4 years; height 1.68 ± 0.09 m; weight 70.2 ± 6.4 kg) were recruited from the Physical Medicine and Rehabilitation Unit of the Scientific Institute of Lissone, S. Maugeri Foundation. All subjects were ensured to be able to follow instructions, to walk independently (with or without walking aids) and to have unilateral lower-limb weakness. Each subject walked at his self-selected speed 12 times over the GaitRite mat, wearing two sensors attached to their shanks. The accuracy and timing agreement for both IC and EC were assessed. The analysis was performed on the whole group of patients who were then divided into three subgroups according to Tilson's classification of impairment [26]: gait speed < 0.4 m/s for patients with severe impairment; 0.4 m/s $<$ gait speed < 0.8 m/s for patients with medium impairment; gait speed > 0.8 m/s for patients with mild impairment.

D. Ethical Approval

All of the experimental protocols were approved by the Institutional Review Board of the Salvatore Maugeri Foundation in Lissone, and the subjects who agreed to participate to the study signed a written informed consent.

III. RESULTS

A. Validation

A representative walking pattern of healthy subjects is illustrated in Fig. 1. Inter-subject and inter-step variability resulted to be low, since the acquired data presented uniform ranges of flexion/extension angle and angular velocity.

A total of 4679 steps were acquired and were then divided into three self-selected speed conditions. Each step included a pair of gait events (IC, EC). The real-time algorithm detected the total amount of IC and EC events, without any false positives. Results are detailed in Table I, reporting the mean speed, the number of steps, and the accuracy (TP, FP, FN, and F1-score).

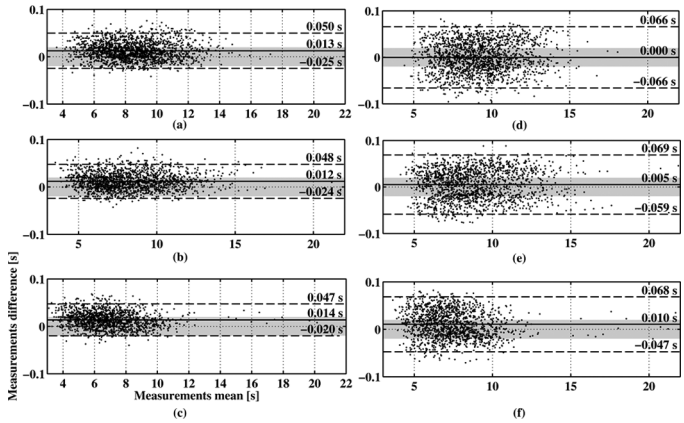

Fig. 2. Bland-Altman plots of Initial Contact (IC) and End Contact (EC), for the slow (panel a, IC; panel d, EC), normal (panel b, IC; panel e, EC), and fast (panel c, IC; panel f, EC) self-selected speeds obtained from the healthy subjects data (N = 22). Positive times correspond to delays in the detection of the real-time algorithm with respect to the GaitRite system. Mean error is reported with a solid horizontal line and limits of agreement (mean ± 1.96 SD) with dashed horizontal lines. Gray area, symmetrical around zero, corresponds to the sampling period of the inertial sensors data (20 ms).

Without the update stage, the performance obtained by the algorithm would have slightly worsened: three false negatives for IC (two for the slow speed, one for the normal speed) and five for EC (two for the slow speed, three for the normal speed) would have been obtained. No false positives would have been collected, resulting in total F1-scores of 0.999 for IC (P = 1, R = 0.999) and 0.999 for EC (P = 1, R = 0.999).

A Bland-Altman plot was obtained for each speed condition and gait event (IC, EC), comparing the real-time algorithm against the GaitRite system (Fig. 2). On each panel, the difference between both methods is plotted against their average. Positive differences correspond to delays in the detection of the real-time algorithm, with respect to the GaitRite system. The mean detection delays [95% confidence interval (CI)] for IC were 12.55 ms [11.65, 13.45] for the slow self-selected speed, 11.91 ms [11.01, 12.81] for the normal self-selected speed and 13.66 ms [12.76, 14.56] for the fast self-selected speed. In the case of EC, the mean detection delays obtained were −0.22 ms [−1.81, 1.37], 5.09 ms [3.49, 6.69], and 10.44 ms [8.89, 11.99], for the slow, normal, and fast self-selected speeds, respectively.

The other algorithms published in the literature [15], [17] tested F1-scores close to 1 for both IC and EC, as reported in Table I. The median and interquartile ranges of the detection delays obtained by the three algorithms are plotted in Fig. 3, for each event and speed condition. The Dunn-Sidak *post hoc* tests ($p < 0.05$) established that for each speed condition and event, all pairs of algorithms were significantly different from each other, with the real-time algorithm always showing the minimum delay.

B. Robustness

1) Influence of Sudden Changes in Pace: The mean velocity change was 0.51 ± 0.24 m/s for the slow-to-fast condition, and −0.57 ± 0.22 m/s for the fast-to-slow condition. The total number of collected steps was 285 for the increasing speed and 306 for the decreasing speed. The overall performance of the

TABLE II
CLINICAL AND DEMOGRAPHIC DETAILS OF THE STROKE PATIENTS

Subject	Age (years)	Sex	Etiology	Paretic side	Time post-stroke	Body Mass Index	Motricity Index (0-100)	Walking Speed (m/s)	Walking aids
S1	74	Male	Ischemic stroke	Right	5 months	25.39	42	0.17 ± 0.02	Walker
S2	67	Female	Hemorrhagic stroke	Right	1 month	26.35	52	0.28 ± 0.03	Walker
S3	86	Female	Ataxic cerebellar stroke	Right	1 month	28.04	63	0.52 ± 0.02	Cane
S4	67	Male	Ischemic stroke	Left	21 days	25.69	52	0.57 ± 0.02	None
S5	89	Male	Ischemic stroke	Left	6 days	21.74	75	0.69 ± 0.06	Cane
S6	63	Female	Ataxic cerebellar stroke	Left	5 months	26.95	75	0.84 ± 0.03	None
S7	60	Male	Ischemic stroke	Left	17 days	27.40	69	0.91 ± 0.07	None
S8	72	Male	Ischemic stroke	Left	2 years	20.52	83	1.17 ± 0.05	None
S9	73	Male	Ataxic cerebellar stroke	Right	1 month	23.62	75	1.19 ± 0.11	Cane
S10	43	Male	Ischemic stroke	Right	7 months	22.69	75	1.38 ± 0.05	None

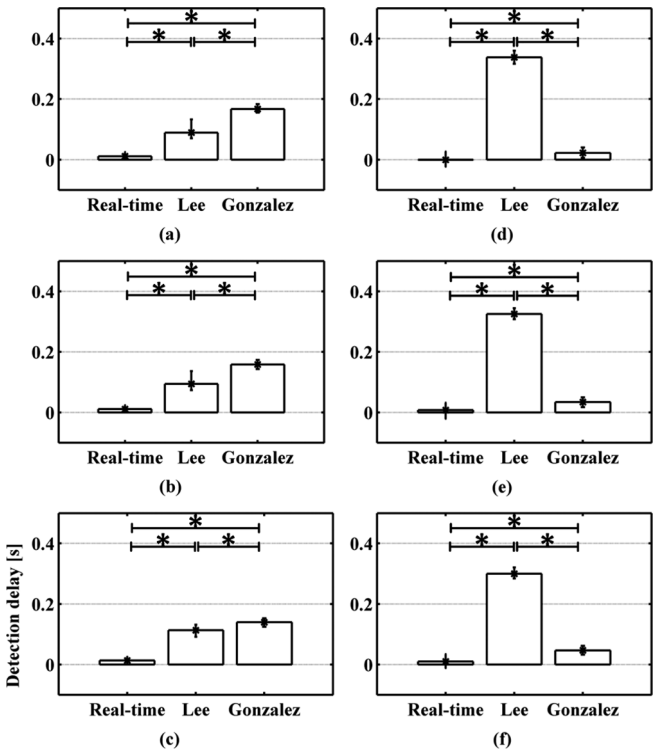

Fig. 3. Algorithms comparison in terms of detection delays for Initial Contact (IC) and End Contact (EC) with respect to the GaitRite system for the slow (panel a, IC; panel d, EC), normal (panel b, IC; panel e, EC), and fast (panel c, IC; panel f, EC) self-selected speeds. Asterisks indicate significant differences (Dunn-Sidak, $p < 0.05$).

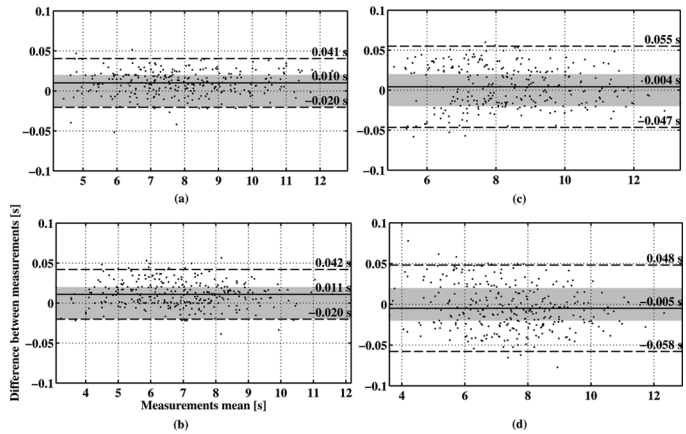

Fig. 4. Bland-Altman plots of the robustness tests on healthy subjects (N = 10), for the IC and EC events at increasing (panel a, IC; panel c, EC) and decreasing (panel b, IC; panel d, EC) speed. Positive times correspond to delays in the detection of the real-time algorithm with respect to the GaitRite system. Mean error is reported with a solid horizontal line and limits of agreement (mean ± 1.96 SD) with dashed horizontal lines. Gray area, symmetrical around zero, corresponds to the sampling period of the inertial sensors data (20 ms).

real-time algorithm reached a total value of F1-score equal to 1, for both IC and EC.

Without the update stage, F1-scores of 0.997 (P = 1, R = 0.993) and 0.992 (P = 1, R = 0.984) would have been obtained for IC at increasing and decreasing speeds, respectively. In the case of EC, the F1-score for increasing speed would have resulted in 0.997 (P = 1, R = 0.993), and 0.985 (P = 1, R = 0.971) for decreasing speed.

The Bland-Altman plots (Fig. 4) showed delays comparable to those obtained from the data of healthy subjects walking at a constant speed (Fig. 2). For the IC detection, the mean delays were 10.09 ms [8.28, 11.90] for the slow-to-fast condition, and 10.97 ms [9.19, 12.75] for the fast-to-slow condition. Whereas for EC the mean errors were 4.25 ms [1.23, 7.27] and −4.87 ms [−7.91, −1.83], for the slow-to-fast and the fast-to-slow conditions, respectively.

2) Influence of Pathological Pattern: Table II shows the main characteristics of the recruited stroke patients, ordered by descending severity of impairment, evaluated in terms of the mean walking speed obtained in the trials. Two patients showed a severe impairment (S1, and S2); three exhibited a medium impairment (S3-S5) and the last five (S6-S10) were characterized by a low level of impairment.

The walking patterns of three subjects representative of the three different levels of impairment are shown in Fig. 5. Panel (a) reports the angular velocity and the flexion/extension angle of three complete strides of a patient with a mild impairment (S7). The subject presented a walking pattern that was quite similar to the one displayed by healthy subjects (Fig. 1), both in terms of peak-to-peak amplitude of the two signals and reduced inter-step variability. It can be observed that the smoothness of the angular velocity diminished, especially during the stance phase of the paretic leg, suggesting a lack of confidence during weight support. This pattern made more difficult the proper detection of the End Contact. Panel (b) shows three complete strides of a subject with a medium level of impairment (S4).

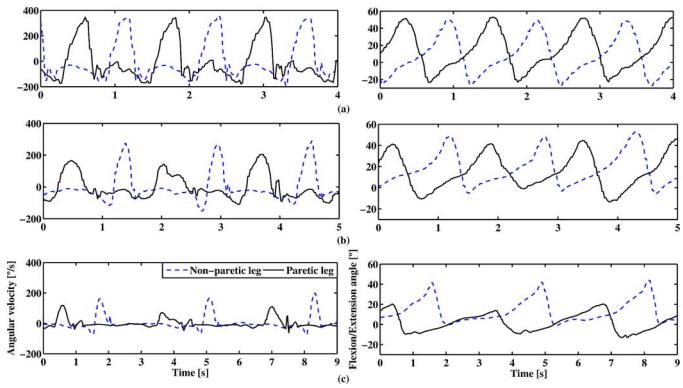

Fig. 5. Walking patterns of three representative stroke patients for mild (panel a, S7), medium (panel b, S4), and severe (panel c, S1) levels of impairment. Both the shank angular velocity (left panels) and the flexion/extension angle (right panels) of the nonparetic (dashed blue) and paretic (solid black) legs are shown. For each subject three complete strides are reported.

The range of the angular velocity notably decreased for the two legs, whereas the inter-step variability increased, mainly for the paretic leg. The amplitude of the flexion/extension angle was also reduced, almost limiting its range to positive values. Therefore, the angle that the shank formed in the sagittal plane with the vertical during IC decreased, thus implying a reduction in the step length. Finally, panel (c) shows three complete strides of a subject with a severe level of impairment (S1), who used a walker during the trial. The amplitude of the angular velocity presented an evident reduction with respect to the medium impairment and a higher inter-leg variability (the double support phase of the paretic leg was 61.60% longer than the nonparetic-leg phase). In addition, the stance phases were characterized by flat and smooth angular velocities, probably due to the support provided by the walker. The bell shape of the angular velocity had a secondary peak at the end of the swing phase, caused by hesitation during the initial contact. The double support phases of the severely impaired subgroup were extended by 54.95% when compared to the healthy subjects (the average increment for all stroke subgroups was 36.48%), with a consequent reduction of the single-leg support phase. The amplitude of the flexion/extension angle of both legs was severely reduced, especially for the paretic leg. Since this angle was defined in the sagittal plane using the vertical as reference, such a reduction in the angle implied a shortening of the step lengths, caused by insecurity during the swing phase.

The accuracy results of the developed algorithm were excellent also with the stroke patients. A total of 1137 steps were recorded, and F1-scores of 0.998 (P $=$ 0.998, R $=$ 0.997) and 0.944 (P $=$ 0.948, R $=$ 0.941) were obtained for IC and EC, respectively. Without the update stage, metrics would have dropped to F1-scores equal to 0.988 (P $=$ 0.999, R $=$ 0.978) and 0.896 (P $=$ 0.909, R $=$ 0.884) for IC and EC, respectively.

Table III reports the accuracy of the real-time algorithm obtained for the subgroups of patients. As foreseeable, the lowest but still highly acceptable accuracy was obtained for the most-impaired group of patients (F1-scores of 0.993 and 0.870 for IC and EC, respectively). Without the update stage the metrics would have slightly worsened for the mild and the medium impaired groups of patients. However, for the most impaired group, F1-scores would have dropped to 0.967 (P $=$ 0.997, R $=$ 0.939) for IC and to 0.726 (P $=$ 0.757, R $=$ 0.697) for EC, demonstrating the usefulness of this stage of the algorithm.

TABLE III
PERFORMANCE OF THE REAL-TIME ALGORITHM IN TERMS OF ACCURACY AND DETECTION DELAYS, OBTAINED SEPARATELY ON THE THREE SUBGROUPS OF STROKE SUBJECTS (MILD, MEDIUM AND SEVERE)

	Initial Contact			End Contact		
	Mild	Med	Severe	Mild	Med	Severe
P	1	1	0.995	0.995	0.961	0.879
R	1	1	0.992	0.995	0.961	0.860
F1	1	1	0.993	0.995	0.961	0.869
Mean Detection Delay (ms) [95% CI]	20.11 [17.62, 22.60]	23.40 [19.70, 27.10]	52.37 [46.50, 58.24]	3.50 [0.32, 6.68]	2.31 [-5.04, 9.66]	15.78 [8.21, 23.35]

The timing delays and limits of agreement are shown in Fig. 6. The mean detection delays were 31.26 ms [28.73, 33.79] for IC, and 6.79 ms [3.48, 10.10] for EC. Different colors and symbols are used to classify patients based on different levels of impairment. The detection delays obtained for the mildly impaired subjects (green triangles, five subjects) were similar to those obtained for the healthy subjects (Figs. 2 and 4). Subjects with medium impairment (yellow circles, three subjects) were characterized by increased discrepancies between the two systems, and in most cases the real-time algorithm detected events earlier than the GaitRite system (especially in the case of EC). Subjects with severe impairment (red squares, two subjects) were characterized by detection delays with the most scattered distribution, thus increasing the limits of agreement.

IV. DISCUSSION

A real-time, adaptive algorithm for gait-event detection was developed and its performance was validated against the GaitRite system, using a dataset of 4679 steps from 22 healthy subjects, aged between 21 and 85 years, who walked at three self-selected speeds (slow, normal and fast). The total set of IC and EC events was correctly identified, reaching F1-scores of 1 for the three speed conditions. The mean detection delays were always below 13.66 ms, suggesting that the algorithm was actually able to identify gait events in real time, obtaining minimum delays with respect to the offline-processed data provided by the GaitRite system.

This dataset was also used to compare the developed algorithm with other two methods already published [15], [17], that used the same inertial and magnetic sensors (MTx sensors from Xsens Technologies B.V) to detect IC and EC. The resultant accuracy metrics were close to 1 also for these algorithms. However, the detection delays obtained by the here-proposed algorithm for all speeds and events were significantly lower than those of the other two algorithms. In particular, Lee's algorithm [17] was affected by a mean detection delay of 104.5 ms for IC and 325.4 ms for EC, which makes it not suitable for real-time applications. These delays were due to the low-pass filter applied to the shank angular velocity and to the choice of the points correlated to the gait events. Indeed, Lee *et al.* defined IC as the minimum of the angular velocity that comes after the maximum

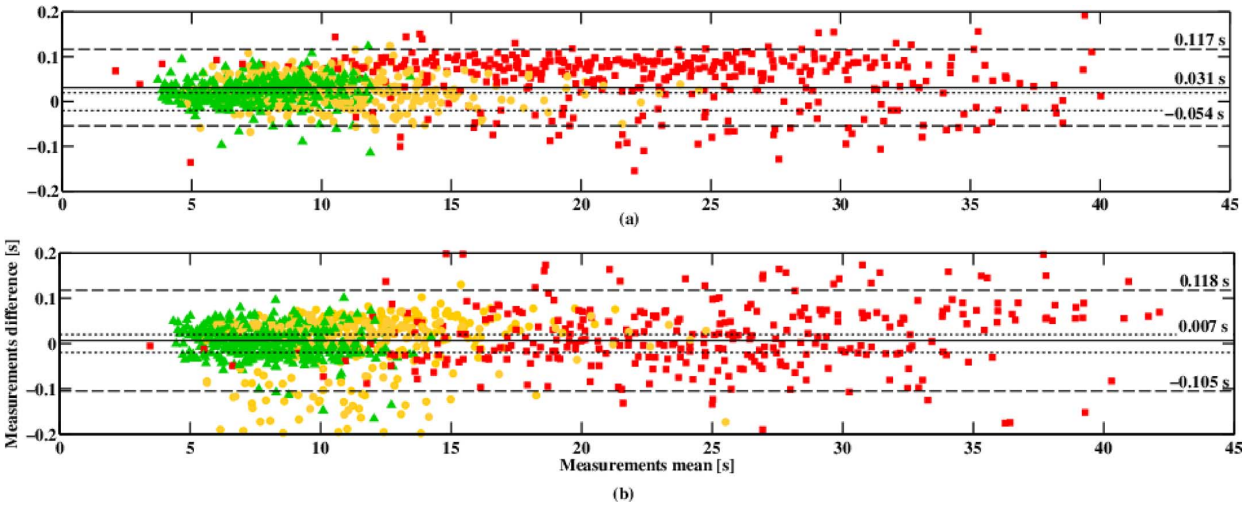

Fig. 6. Bland-Altman plots of the robustness validation with stroke subjects (N = 10) for the IC (a) and EC (b) events. Positive times correspond to delays in the real-time algorithm with respect to the GaitRite system. Mean error is reported with a solid horizontal line and limits of agreement (mean ± 1.96 SD) with dashed horizontal lines. Dotted lines delimit the area corresponding to the sampling period of the inertial sensors data (20 ms). Patients with different levels of impairment are shown in different colors: green triangles (mild impairment), yellow circles (medium impairment), and red squares (severe impairment).

peak (MS, in Fig. 1), whereas we preferred to identify IC as the minimum of the flexion/extension angle, since we observed that this point was better synchronized with the IC event detected by the GaitRite system. The detection delay of Lee's algorithm increased even more significantly in the case of EC, since the identification of MS triggered the search of a past EC event. González's algorithm [15] was based on the acceleration signals acquired from a sensor placed on the S1 vertebra. Low-pass filters with narrow pass-bands were applied, resulting in mean detection delays of 157.2 ms for IC and 37.4 ms for EC. The use of a single sensor increases system portability and is more cost effective, but also reduces the available information being processed, making it difficult to analyze asymmetric walking patterns.

The algorithms proposed by Lee and Gonzalez were reproduced by the authors in order to allow a quantitative comparison on the same dataset, since the algorithms were based on a minimal number of sensors and were implemented in real time, as the one proposed by the authors. However, other methods have been published in the literature. Rueterbories *et al.* developed a real-time algorithm to detect gait events from the radial and tangential accelerations of the foot, which was validated on healthy subjects and stroke patients [18]. The authors achieved levels of accuracy similar to those of the here-proposed algorithm, but the timing disagreement between the real-time detection and the reference system (footswitches) had a higher variability. Kotiadis *et al.* proposed different algorithms to detect IC and EC using an inertial sensor placed on the shank, whose signals were processed offline to assess which method was best to be implemented online [16]. Their final algorithm, using offline bidirectional filtering and manually set thresholds, achieved a high level of accuracy in one stroke subject walking over various surfaces; nevertheless, a further validation with more subjects and a real-time implementation of the filter is needed. Hanlon *et al.* detected IC on 12 healthy subjects simulating different walking patterns, obtaining mean absolute errors of 9.5 ± 9.0 ms [19]. However, they used two accelerometers placed on the knee and ankle joints instead of a single sensor per leg, detected a single event, and did not provide a validation on neurological patients. McCamley *et al.* extracted the IC and EC using a waist-mounted inertial sensor that was processed with the continuous wavelet transform, obtaining very good results and detection delays for young and healthy subjects, which were comparable to those obtained by the presented real-time algorithm [20]. Further studies should assess its applicability to nonasymmetric patterns, typical of some pathologic patients, and the feasibility of performing the continuous wavelet transform in real time.

Two additional datasets were acquired to verify the algorithm robustness. The first one tested the performance of the developed algorithm against sudden speed changes, resulting in F1-scores equal to 1 for all events (IC, EC) and speed conditions (increasing and decreasing speeds). Detection delays were comparable to those obtained for healthy subjects walking at a constant speed, suggesting that the rapid adaptability of the algorithm makes it suitable for long-term, daily-life acquisitions, free from the enclosed walkway of the GaitRite system.

The performance of the algorithm was also assessed on walking patterns acquired from a group of stroke patients (N = 10). The recruited patients were very heterogeneous in terms of etiology, time elapsed since stroke and level of impairment (walking speeds ranged from 0.17 to 1.38 m/s), in order to provide a more extensive robustness validation of the algorithm. Some of the patients used aids during the trials, such as canes or walkers. The real-time algorithm provided excellent results when applied to stroke subjects, with F1-scores of 0.998 for IC and 0.944 for EC. Mean detections delays were 31.26 ms for IC and 6.79 ms for EC. Due to the higher inter-step variability that the stroke patients presented with respect to the healthy subjects, the update stage of the algorithm was crucial in achieving this level of performance.

In order to assess the relationship between the algorithm performance and the level of impairment, the dataset acquired from stroke patients was divided in three subgroups, based on the

walking speed [26]. However, the low number of subjects within each group (especially for the most severely impaired) limited the possibility of drawing any final comments. The results obtained from subjects belonging to the groups with medium and mild levels of impairment (walking speed > 0.4 m/s) were similar to those obtained from healthy subjects. A slight decrease in the performance was reported for subjects with severe impairment (walking speed < 0.4 m/s), with F1-scores values of 0.993 for IC and 0.869 for EC. The walking patterns of the two severely impaired subjects were affected by a high level of inter-step variability (Fig. 5), nevertheless the mean detection delays achieved were 52.37 ms for IC and 15.78 ms for EC.

The algorithm was tested only on hemiparetic gait patterns; future research should consider the extension of the dataset, including subjects affected by other neurological diseases, such as SCI, Parkinson Disease, or Multiple Sclerosis. In addition, other tests could include daily-life acquisitions, assessing the robustness against more abrupt changes in gait speed and non-straight walking trajectories. Another limitation of the study is that the algorithm was based on drift-free accelerations, angular velocities, and orientation matrices provided by the Kalman filter embedded in the MTx sensors (Xsens Technologies B.V). Since this filter also uses the information provided by the magnetometers, an environment free from magnetic disturbances was required to avoid measurement interferences. Furthermore, the use of a filter embedded in a commercial-type sensor implies that the algorithm is not immediately exportable to other IMMSs. The Kalman filter also limited the sampling frequency, which was finally set to 50 Hz in order to simultaneously use three sensors. Even though it is sufficient for gait acquisitions, it is very likely that a higher sampling frequency could have additionally reduced the detection delays; nevertheless, studies should be carried out to analyze these effects.

In conclusion, a real-time, adaptive algorithm for gait-event detection was validated against the GaitRite system on healthy subjects (N $= 22$, aged 21 to 85 years old) and on a heterogeneous group of patients with hemiparesis (N $= 10$). The validation was designed in order to replicate a realistic clinical use. Therefore, the experiments were performed on different days, the sensors were placed by four different operators, and the subjects were asked to walk barefoot if they were wearing heeled shoes or clogs. The sensors were placed on the external part of both shanks but no special attention was required. Naturally, sensors misplacement might introduce systematic errors in the signals acquired, but this would not necessarily affect the performance of the algorithm. Indeed, the initial procedure to compensate for misalignments between the sensor and the longitudinal axis of the shank, the subject-specific calibration of the thresholds and the update stage maximize the detection accuracy. The designed algorithm reliably identified six gait phases in real time, thus providing an extensive knowledge about the gait cycle which would not be available in real time if only using the GaitRite system. This knowledge can be used for the design of advanced closed-loop control systems for Functional Electrical Stimulation or biofeedback controllers synchronized with gait training, which may improve the efficacy of gait interventions for neurological patients.

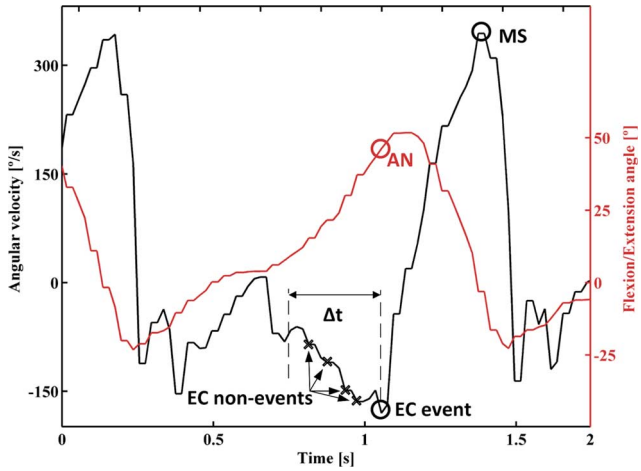

Fig. 7. Peaks of interest for the definition of the EC threshold, extracted from the shank angular velocity and flexion/extension angle of the paretic leg of a stroke subject with mild impairment (S7). MS, AN and EC events are shown. EC non-events are the peaks of the angular velocity signal that could be misdetected as the EC event, which are located in the time interval $\Delta t = [\mathrm{tEC} - (\mathrm{tMS} - \mathrm{tEC}); \mathrm{tEC}]$.

APPENDIX

The detection stage of the algorithm extracted the gait events by finding peaks located in the corresponding gait state, comparing their amplitude with a predetermined threshold. Four thresholds were used for EC, AN, MS, and IC. These thresholds were initialized in the calibration stage using data acquired from five steps, and then updated every step (update stage).

In the following, we refer to the outputs of the first order filter (detection stage) as real-time signals and to the outputs of the 10th order filter (update stage) as quasi real-time signals. The thresholds defined for the real-time and the quasi real-time signals are then referred to as real-time and quasi real-time thresholds.

EC was defined as the minimum of the angular velocity that happens before MS. In the detection stage, the search of EC started when the real-time flexion/extension angle signal exceeded the AN real-time threshold; then, the algorithm looked for a minimum whose amplitude was lower than the EC real-time threshold. Such a threshold was needed to distinguish the EC event from the other local minima (EC non-events) located before it, at the end of the stance phase (see Fig. 7). This threshold was computed in the update stage, using the quasi real-time angular velocity: the EC event was reliably identified as the negative minimum of the quasi-real time signal before the MS event, and then the corresponding minimum on the real-time signal was tagged as EC event; all the other local minima within the time interval $[t_{\mathrm{EC}} - (t_{\mathrm{MS}} - t_{\mathrm{EC}}); t_{\mathrm{EC}}]$ were tagged as EC non-events. Since at the end of the stance phase the angular velocity signal was a negative, decreasing function, the real-time threshold was defined as the mean between the minimum amplitude of the EC peaks classified as non-events for the last five steps and the maximum amplitude of the EC peaks classified as events for the last five steps.

AN was introduced to facilitate the detection of EC, particularly in the case of pathological gait patterns, since there were some local minima before EC (EC non-events) that could be

misclassified as gait events. AN was defined as the flexion/extension angular value corresponding to the time instant of EC, and the set of AN values of the last five steps was used to create a threshold that started the search of EC. Since in the proximity of EC the flexion/extension angle was an increasing function, the real-time threshold for AN was computed as the mean between the minimum amplitude of the AN corresponding to the last five EC events and the maximum amplitude of all the other AN values associated to the EC non-events collected from the previous five steps.

MS was defined as the maximum of the angular velocity signal. In the detection stage, MS was identified as the peak of the angular velocity whose amplitude exceeded a certain threshold. This threshold was computed during the update stage, applying Otsu's thresholding method [27] to the quasi real-time angular velocity signal. Otsu's method is typically used in image processing to convert a gray-level image to black and white. This method assumes the existence of two classes of points (black and white) and calculates the optimal threshold that maps gray levels to black and white, minimizing intraclass variance. This is done by finding the optimal threshold k* that maximizes the between-class variance (σ_B^2) defined as follows:

$$\sigma_B^2 = \frac{\left[\mu_{\mathrm{T}}\omega\left(k\right) - \mu\left(k\right)\right]^2}{\omega\left(k\right)\left[1 - \omega\left(k\right)\right]} \tag{2}$$

where $\omega(\mathrm{k})$ and $\mu(\mathrm{k})$ are the zeroth- and the first-order cumulative moments of the histogram up to the kth level of intensity. μ_{T} is the mean level of the total set of points.

Its advantage, when applied to the proposed algorithm, is that the Otsu's method was able to automatically separate the MS events from other maxima of the angular velocity (MS non-events), exploiting the variability between events and non-events. To identify the MS quasi real-time threshold, all the maxima of the quasi real-time angular velocity of the last five steps were collected. For positive maxima, the positive area under the curve around the peak was computed, whereas for negative maxima the value was set to zero. The Otsu's method was applied to this dataset, computing a threshold that divided the peaks of the quasi real-time angular velocity into MS events and non-events. Then, for each point, the corresponding maximum on the real-time signal was analogously classified as event or non-event. The MS real-time threshold was computed as the mean between the maximum amplitude of the MS peaks classified as non-event and the minimum amplitude of the MS peaks classified as events.

Finally, IC was identified as the minimum of the flexion/extension angle whose amplitude was lower than the related threshold. In the update stage, the minima of the quasi real-time flexion/extension angle of the last five steps were collected; then, the corresponding events were located on the real-time signal, and the real-time IC threshold was computed as mean + $3 \cdot$standard deviations in order to take into account the quasi-totality (i.e., 99.7%) of the collected peaks.

REFERENCES

[1] J. J. Daly and R. L. Ruff, "Construction of efficacious gait and upper limb functional interventions based on brain plasticity evidence and model-based measures for stroke patients," *Scientific World J.*, vol. 7, pp. 2031–2045, 2007.

[2] S. Ferrante, E. Ambrosini, P. Ravelli, E. Guanziroli, F. Molteni, G. Ferrigno, and A. Pedrocchi, "A biofeedback cycling training to improve locomotion: A case series study based on gait pattern classification of 153 chronic stroke patients," *J. Neuroeng. Rehabil.*, vol. 8, p. 47, 2011.

[3] J. Jonsdottir, D. Cattaneo, M. Recalcati, A. Regola, M. Rabuffetti, M. Ferrarin, and A. Casiraghi, "Task-oriented biofeedback to improve gait in individuals with chronic stroke: Motor learning approach," *Neurorehabil. Neural Repair*, vol. 24, no. 5, pp. 478–485, Jun. 2010.

[4] L. R. Sheffler and J. Chae, "Neuromuscular electrical stimulation in neurorehabilitation," *Muscle Nerve*, vol. 35, no. 5, pp. 562–590, May 2007.

[5] R. Dickstein, "Rehabilitation of gait speed after stroke: A critical review of intervention approaches," *Neurorehabil. Neural Repair*, vol. 22, no. 6, pp. 649–660, Dec. 2008.

[6] E. Ambrosini, S. Ferrante, G. Ferrigno, F. Molteni, and A. Pedrocchi, "Cycling induced by electrical stimulation improves muscle activation and symmetry during pedaling in hemiparetic patients," *IEEE Trans. Neural Syst. Rehabil. Eng.*, vol. 20, no. 3, pp. 320–330, May 2012.

[7] J. Rueterbories, E. G. Spaich, B. Larsen, and O. K. Andersen, "Methods for gait event detection and analysis in ambulatory systems," *Med. Eng. Phys.*, vol. 32, no. 6, pp. 545–552, Jul. 2010.

[8] K. Aminian, B. Najafi, C. Büla, P.-F. Leyvraz, and P. Robert, "Spatio-temporal parameters of gait measured by an ambulatory system using miniature gyroscopes," *J. Biomech.*, vol. 35, no. 5, pp. 689–699, May 2002.

[9] C. C. Monaghan, W. J. B. M. van Riel, and P. H. Veltink, "Control of triceps surae stimulation based on shank orientation using a uniaxial gyroscope during gait," *Med. Biol. Eng. Comput.*, vol. 47, no. 11, pp. 1181–1188, Nov. 2009.

[10] P. Picerno, A. Cereatti, and A. Cappozzo, "Joint kinematics estimate using wearable inertial and magnetic sensing modules," *Gait Posture*, vol. 28, no. 4, pp. 588–595, Nov. 2008.

[11] K. Saber-Sheikh, E. C. Bryant, C. Glazzard, A. Hamel, and R. Y. W. Lee, "Feasibility of using inertial sensors to assess human movement," *Man. Ther.*, vol. 15, no. 1, pp. 122–125, Feb. 2010.

[12] A. G. Cutti, A. Ferrari, P. Garofalo, M. Raggi, A. Cappello, and A. Ferrari, "'Outwalk': A protocol for clinical gait analysis based on inertial and magnetic sensors," *Med. Biol. Eng. Comput.*, vol. 48, no. 1, pp. 17–25, Jan. 2010.

[13] J.-A. Lee, S.-H. Cho, Y.-J. Lee, H.-K. Yang, and J.-W. Lee, "Portable activity monitoring system for temporal parameters of gait cycles," *J. Med. Syst.*, vol. 34, no. 5, pp. 959–966, Oct. 2010.

[14] A. Mansfield and G. M. Lyons, "The use of accelerometry to detect heel contact events for use as a sensor in FES assisted walking," *Med. Eng. Phys.*, vol. 25, no. 10, pp. 879–885, Dec. 2003.

[15] R. C. González, A. M. López, J. Rodriguez-Uría, D. Alvarez, and J. C. Alvarez, "Real-time gait event detection for normal subjects from lower trunk accelerations," *Gait Posture*, vol. 31, no. 3, pp. 322–325, Mar. 2010.

[16] D. Kotiadis, H. J. Hermens, and P. H. Veltink, "Inertial gait phase detection for control of a drop foot stimulator inertial sensing for gait phase detection," *Med. Eng. Phys.*, vol. 32, no. 4, pp. 287–297, May 2010.

[17] J. K. Lee and E. J. Park, "Quasi real-time gait event detection using shank-attached gyroscopes," *Med. Biol. Eng. Comput.*, vol. 49, no. 6, pp. 707–712, Jun. 2011.

[18] J. Rueterbories, E. G. Spaich, and O. K. Andersen, "Gait event detection for use in FES rehabilitation by radial and tangential foot accelerations," *Med. Eng. Phys.*, Oct. 2013.

[19] M. Hanlon and R. Anderson, "Real-time gait event detection using wearable sensors," *Gait Posture*, vol. 30, no. 4, pp. 523–527, Nov. 2009.

[20] J. McCamley, M. Donati, E. Grimpampi, and C. Mazzà, "An enhanced estimate of initial contact and final contact instants of time using lower trunk inertial sensor data," *Gait Posture*, vol. 36, no. 2, pp. 316–318, Jun. 2012.

[21] N. Chia Bejarano, E. Ambrosini, A. Pedrocchi, G. Ferrigno, M. Monticone, and S. Ferrante, L. M. Roa Romero, Ed., "An adaptive real-time algorithm to detect gait events using inertial sensors," in *Proc. XIII Mediterranean Conf. Medical and Biological Engineering Computing*, 2014, pp. 1799–1802.

[22] J. K. Lee and E. J. Park, "3D spinal motion analysis during staircase walking using an ambulatory inertial and magnetic sensing system," *Med. Biol. Eng. Comput.*, vol. 49, no. 7, pp. 755–764, Jul. 2011.

[23] K. E. Webster, J. E. Wittwer, and J. A. Feller, "Validity of the GAITRite walkway system for the measurement of averaged and individual step parameters of gait," *Gait Posture*, vol. 22, no. 4, pp. 317–321, Dec. 2005.
[24] R. G. Cutlip, C. Mancinelli, F. Huber, and J. DiPasquale, "Evaluation of an instrumented walkway for measurement of the kinematic parameters of gait," *Gait Posture*, vol. 12, no. 2, pp. 134–138, Oct. 2000.
[25] J. M. Bland and D. G. Altman, "Statistical methods for assessing agreement between two methods of clinical measurement," *Lancet*, vol. 1, no. 8476, pp. 307–310, Feb. 1986.
[26] J. K. Tilson, K. J. Sullivan, S. Y. Cen, D. K. Rose, C. H. Koradia, S. P. Azen, and P. W. Duncan, "Meaningful gait speed improvement during the first 60 days poststroke: Minimal clinically important difference," *Phys. Ther.*, vol. 90, no. 2, pp. 196–208, Feb. 2010.
[27] N. Otsu, "A Threshold selection method from gray-level histograms," *IEEE Trans. Syst. Man Cybern.*, vol. 9, no. 1, pp. 62–66, Jan. 1979.